

博士論文要旨

機械学習を用いた多方向光学式骨密度計測法の開発

DEVELOPMENT OF A MULTIDIRECTIONAL OPTICAL BONE DENSITOMETRY USING MACHINE LEARNING TECHNIQUES

三浦 要

金沢大学大学院自然科学研究科機械科学専攻

主任指導: 田中 茂雄
提出日: 2022 年 6 月 20 日

Abstract

To achieve early detection of osteoporosis, a simple bone densitometry method using optics was proposed. However, individual differences in soft tissue structure and optical properties can cause errors in quantitative bone densitometry. Therefore, developing optical bone densitometry that is robust to soft tissue variations is important for the early detection of osteoporosis. The purpose of this study was to develop an optical bone densitometry that is robust to soft tissue using machine learning techniques and to verify its feasibility using Monte Carlo simulations. We proposed a method to measure spatially resolved diffuse light from three directions of a tissue and used machine learning techniques to predict bone density from these data. Here, the three directions were backward, forward, and lateral to the direction of ballistic light irradiation. For the biological tissue, synthetic biological tissue models with 1211 different random structural and optical properties were used. Trabecular bone tissue in the synthetic biological tissue model was generated by a reaction-diffusion model. The training data for the machine learning model were the results of Monte Carlo simulations on synthetic biological tissue models. The results were computed after a 10-fold cross-validation. From the simulated optical data, the machine learning model predicted bone density with a coefficient of determination of 0.760. The optical bone densitometry method proposed in this study was found to be robust against individual differences in soft tissue.

1. Introduction

X-ray is used for osteoporosis diagnosis, including dual energy X-ray absorptiometry (DXA).¹ However, it is difficult to utilize these devices for the early detection of osteoporosis, which only has a moderate decrease in bone mineral density (BMD), due to their large size and potential harmfulness, indicating the necessity for a compact and safe device for screening of osteoporosis. Near-infrared light is useful for non-invasive measurement of different types of bio-information and is utilized in the medical field. Bone densitometry using near-infrared light could be a new screening method for osteoporosis, however, quantitative measurement of BMD in the near-infrared wavelength range is difficult because of variations in soft tissue structure and optical properties due to individual differences.²⁻⁴ we propose a multi-directional optical bone densitometry. This system realizes optical bone densitometry robust to individual differences in soft tissue thickness and color by using machine learning techniques and spatially resolved steady-state scattered light data acquired from three directions of the tissue relative to the light irradiation direction: back, forward, and lateral. The purpose of this study is to develop a multi-directional optical bone densitometry method using machine learning and to validate its effectiveness by Monte Carlo simulations. If this method is sufficiently accurate, it can be used for simple and safe bone densitometry, thus contributing to the early detection of osteoporosis.

2. Materials and methods

Simulation data for the multi-directional optical bone densitometry method was obtained by performing Monte Carlo simulations on a virtually synthesized biological tissue model and using the results as training data for the machine learning model. The simulation was performed in the following five steps as shown in Fig. 1.

Step 1, the biological tissue model was synthesized by the following three procedures. First, the structural properties of the biological tissue model were determined randomly. The structural properties of the biological tissue models are listed in Table 1. The thicknesses of the dermis and the subcutaneous tissue were determined using random numbers of uniform probability with a range of 1–2 mm and 1–6 mm respectively.^{5,6} The structural properties of the bone tissue were based on measurements of the ultra-distal radius of women by Boutroy (2005) et al.⁷ The cortical bone thickness (C.Th) and trabecular bone volume (BV) fraction (BV/tissue volume (TV)) vary at different stages of osteoporosis (osteoporosis, osteopenia, and healthy subjects). Therefore, the C.Th and BV/TV were determined using random numbers, assuming a normal distribution with different mean and variance values for each stage of osteoporosis. The distributions of C.Th and BV/TV were correlated with a Pearson correlation coefficient r of 0.54. The BMD of bone matrix (mBMD) assumed 1.2 g/cm^3 of fully calcified bone. Second, the trabecular bone tissue

model was generated by defining the trabecular pattern with Turing's reaction-diffusion model⁸ and binarizing the trabecular bone and the gap with a threshold value of u_{th} . Here, the size of one voxel l_v comprising the model was set to $24.5 \mu\text{m}$. This model can define trabecular bone with different BV/TV by changing the u_{th} . Morphometric measurements such as BV/TV, number of trabeculae (Tb.N), trabecular width (Tb.Th), fractal dimension, and structure model index (SMI) of the generated trabecular bone model were consistent with the actual trabecular bone of the ultra-distal radius. Third, cortical bone, subcutaneous tissue and dermis were generated at defined thicknesses in the outward direction of the bone tissue (Fig. 1). When generating cortical bone, the cortical bone surface was adjusted so that each side was 17.15 mm . All the above processes were coded in Python 3.8.

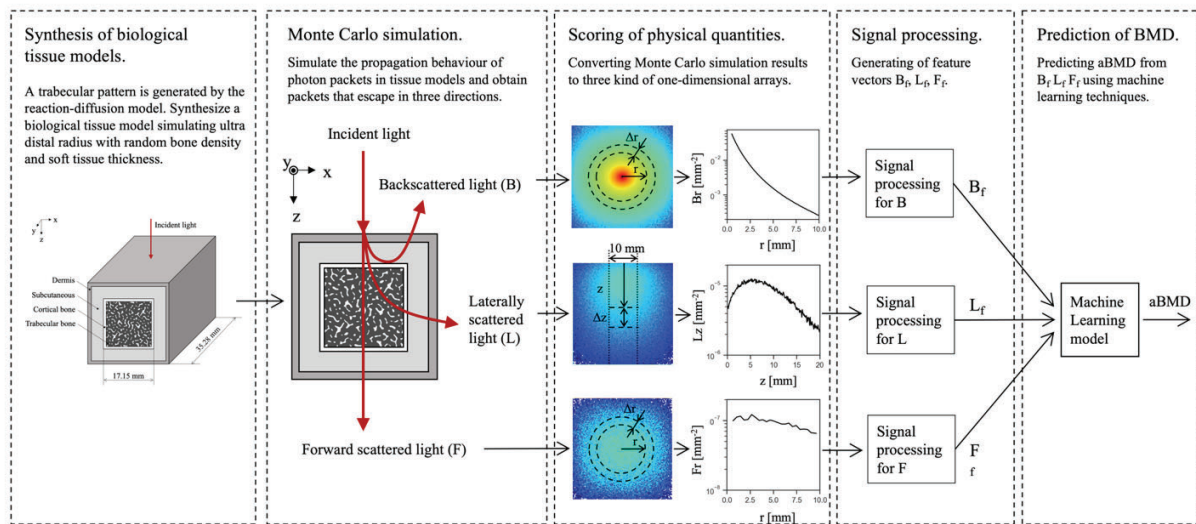


Fig. 1 Bone density prediction procedure by machine learning model using Monte Carlo simulation data

Table 1 Structural properties of biological tissue models.

	Thickness in z and x-axis direction [mm]	BV/TV	mBMD [g/cm ³]	Ref
Dermis	1.0–2.0	-	-	Kozarova (2017) ⁵
Subcutaneous	1.0– 6.0	-	-	Hassager (1989) ⁶
Cortical bone	Osteoporosis 0.487 ± 0.138 , Osteopenia 0.571 ± 0.173 , Normal 0.804 ± 0.149 .	-	1.2	Boutroy (2005) ⁷
Trabecular bone	17.15 minus the cortical bone thickness	Osteoporosis 8.5 ± 2.2 , Osteopenia 10.3 ± 3.0 , Normal 13.4 ± 2.8 .	1.2	Boutroy (2005) ⁷

The values showing the range (number - number) have a uniform distribution of probability, and the mean \pm standard deviation has a normal distribution. The three states of cortical bone thickness and BV/TV correspond to their respective values.

Step 2. Light transport in the synthetic biological tissue model was simulated using the Monte Carlo method. To deal with a tissue model containing trabecular bone with a three-dimensional nonlinear pattern (Fig1), a voxel-based Monte Carlo simulation (VMC) was built by extending the Monte Carlo model for steady-state light transport in multilayered tissues (MCML)⁹ to three dimensions. To represent individual differences, the optical properties of soft tissues were randomly determined (Table 2). The range of optical properties was determined by referring to literature values, assuming measurements with ballistic light at a wavelength of 850 nm. μ_a and μ_s of the soft tissue were determined using the measurements of Simpson (1998) et al.¹⁰ with uniform random numbers. The optical properties of the dermis measured by Simpson included those of negroid and caucasoid, and they assumed that the dermis and epidermis were combined. Most of the bone marrow in the radius is composed of adipose cells after the age of 20 to 30 years.¹¹ Therefore, the optical properties of the bone marrow are the same as those of the subcutaneous tissue, which is mainly composed of adipocytes. Monte Carlo simulation were performed with a total photon count N of 10^7 . VMC was applied to 1211 tissue models with different structural and optical properties. In each model, the structural and optical properties were randomly combined in the ranges listed in Tables 1 and 3. Photon packets that escaped from the tissue model were categorized as backward, forward, or lateral to the direction of the packets launched. For the lateral direction, only the positive direction of the x-axis was considered. Photon packets escaping in three directions were defined as backscattered light (B), forward scattered light (F), and lateral scattered light (L).

Table 2 Optical properties of biological tissue models.

	μ_a [mm^{-1}]	μ_s [mm^{-1}]	g	n	Ref
Dermis	0.0063 - 0.0856	14.20 - 25.06	0.9	1.4	Simpson (1998) ¹⁰
Subcutaneous	0.0049 - 0.0124	8.30 - 13.96	0.9	1.4	Simpson (1998) ¹⁰
Bone	0.0237	20.58	0.9	1.55	μ_a and μ_s , Ugryumova (2004) ¹² ; n , Ascenzi (1959) ¹³ .

μ_a , absorption coefficient; μ_s , scattering coefficient; g , anisotropy coefficient; n , refractive index.

Step 3, the physical quantity of packets escaping in the three directions was scored. For B and F , the sum of photon weights w was calculated for each radial distance r from the photon packet launched coordinate with a range of Δr , as shown in Fig. 1. For L , the sum of photon weights w was calculated for each positive distance along the z -axis from the photon packet irradiation coordinate with a range Δz , as shown in Fig. 1. Scored B , F , and L were B_r , F_r , and L_z , respectively.

Step 4, the obtained B_r , F_r , and L_z were processed to generate the feature vectors B_f , F_f and L_f . The feature vectors B_f , F_f , and L_f are

$$B_f = [B_r, \ln mB_r, \ln vB_r] \quad (1)$$

$$F_f = [\ln mF_r, \ln vF_r] \quad (2)$$

$$L_f = [\ln L_z, \ln mL_z, \ln vL_z] \quad (3)$$

where mB_r , mF_r , and mL_r are the mean, and vB_r , vF_r , and vL_r are the variances of B_r , F_r , and L_r , respectively. F_r was not used in F_f because F_r did not form a valid distribution. The elements of each feature vector were normalized to a mean of 0 and standard deviation (SD) of 1 for the dataset.

Step 5, the machine learning module was used to predict areal BMD (aBMD) of the synthetic biological model. Support Vector Regression (SVR) was used for the module that infers the function that relates the feature vectors (B_f , F_f , L_f) to aBMD from the labeled examples. SVR is less sensitive to noise by using ϵ -insensitive loss functions and can construct nonlinear functions using kernel tricks.¹⁴ A radial basis function (RBF) kernel was selected and tested with the kernel coefficient γ varying in the range of 10^{-4} to 1. The soft margin C and tube ϵ were also adjusted. For SVR, we used the modules included in scikit-learn 0.24.2.

To select the best structure and parameters for SVR module, 80% of the total data were used as a training and validation dataset (trDataset). The remaining 20% of the dataset (tsDataset) was used for testing and comparison purposes. The structure and parameter set of each algorithm were modified, and the best performing one was selected after a 10-fold cross-validation with grid search in trDataset. In 10-fold cross-validation, 90% of the dataset was randomly selected and used for training, and the rest were used for validation. This was performed 10 times by rotating the dataset. The stability of the ML techniques was also verified by cross-validation. After obtaining the best configuration, tsDataset was used to evaluate the performance. The coefficient of determination (r^2) was used as the metric for performance evaluation.

3. Results and discussion

The performance of the system was tested on all 1211 data cases using the SVR method. The relationship between the predicted and reference values of aBMD is shown in Fig. 2. A linear regression of predicted and reference aBMD yielded an r^2 value of 0.760, indicating reasonable agreement. This result suggest that BMD can be predicted with high accuracy using this method, even if there is variance in the thickness and optical properties of the soft tissue.

Because the biological tissue model synthesized in this study is randomly constructed based on the range that a living organism can exhibit, the data obtained by the Monte Carlo simulation is considered to reflect a population with sufficient variance. The range of soft tissue properties was determined randomly

based on measurements. In particular, the optical properties of the dermis cover a wide range of people, from colored individuals to Caucasians¹⁰. In bone tissue, a trabecular pattern was generated by the reaction-diffusion model, because it is difficult to assign the trabecular bone a single scattering coefficient representative of a BMD value. The equation of Ugryumova¹² yields negative scattering coefficients for a range of trabecular bone BMDs. In addition, Pifferi et al. found no age-related changes in the scattering coefficient in calcaneal measurements using TSR.⁴ Overall, the unique and irregular shape of the trabecular pattern may lead to a different light scattering process compared to a homogeneous medium. The trabecular patterns generated in this study were similar to those of real bone in terms of appearance, BV/TV, and quantitative geometric structure. Additionally, BMD was randomly adjusted from severe osteoporosis to the range of normal subjects. Moreover, the Monte Carlo method is the gold standard for modeling light transport in tissues.⁴⁹ Therefore, we consider that the diffuse light simulated in this study represents the structural and optical properties of the biological tissue for a population of sufficient variance.

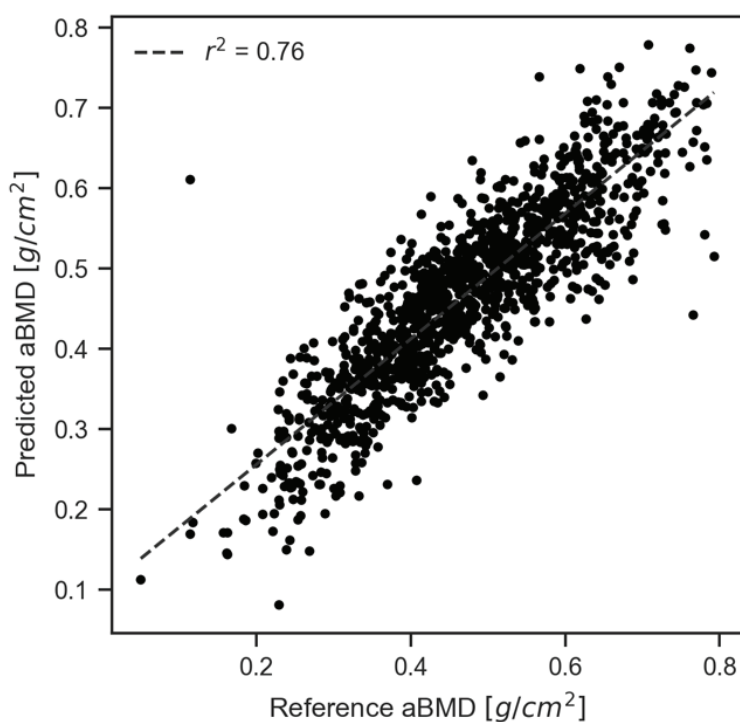


Fig. 2 Relationship between predicted and reference aBMD.

There are several limitations to this study. First, the simulation was only a theoretical test. However, the simulations provide theoretical and clear insights into the different tissues that affect diffuse light. In addition, we believe that the combination of Monte Carlo simulation and ML techniques has several

implications for the development of non-invasive medical measurements using the light diffusion theory that are beyond theoretical verification. An ML model built with sufficient variance and a large amount of data has excellent generalization performance; however, in the field of medical measurement, there are often ethical barriers and difficulties in data acquisition, such as a limited number of cases and invasive measurements. The simulation, which can generate almost unlimited data if computational resources are available, could offer a promising solution to such problems. Second, a simple rectangular biological tissue model was adopted in this study. This model did not consider the heterogeneity in soft tissues, blood vessels, and complex bone structures; however, this information could be implemented in the model using CT and MRI techniques. However, the potential importance of this model is that it allows for a simple and targeted discussion of random changes in soft tissue thickness and optical properties in the validation of optical bone densitometry. This model might provide useful information about the interaction between the bone and soft tissue in measurements using diffuse light. All the limitations mentioned here are attributed to the fact that it is unclear how much of the actual biological tissue should be assumed in the model to represent the light diffusion phenomenon and its output in vivo. It is also possible that simpler models represent substantial physical phenomena. Therefore, it is necessary to verify this by model experiments using phantoms.

4. Conclusion

In this study, a multi-directional optical bone densitometry method using machine learning techniques was developed and validated by simulation. From the results obtained, we conclude that aBMD predicted from spatially resolved steady-state diffuse light data acquired in the posterior, anterior, and lateral planes of the biological tissue model is robust to differences in soft tissue layer thickness and optical properties.

References

1. El Maghraoui, A. & Roux, C. DXA scanning in clinical practice. *Qjm* **101**, 605–617 (2008).
2. Chung, C., Chen, Y. P., Leu, T. H. & Sun, C. W. Near-infrared bone densitometry: A feasibility study on distal radius measurement. *J. Biophotonics* **11**, 1–5 (2018).
3. Miura, K., Matsubara, H. & Tanaka, S. M. Development of optical bone densitometry using near-infrared light. *J. Mech. Eng.* **5**, 60–67 (2018).
4. Pifferi, A. *et al.* Optical biopsy of bone tissue: a step toward the diagnosis of bone pathologies. *J. Biomed. Opt.* **9**, 474 (2004).
5. Kozarova, A., Kozar, M., Minarikova, E. & Pappova, T. Identification of the Age Related Skin Changes Using High-Frequency Ultrasound. *Acta Medica Martiniana* **17**, 15–20 (2017).
6. Hassager, C., Borg, J. & Christiansen, C. Measurement of the subcutaneous fat in the distal forearm by single photon absorptiometry. *Metabolism* **38**, 159–165 (1989).
7. Boutroy, S., Bouxsein, M. L., Munoz, F. & Delmas, P. D. In vivo assessment of trabecular bone microarchitecture by high-resolution peripheral quantitative computed tomography. *J. Clin. Endocrinol. Metab.* **90**, 6508–6515 (2005).
8. Turing, A. M. The chemical basis of morphogenesis. *Philos. Trans. R. Soc. Lond. B. Biol. Sci.* **237**, 37–72 (1952).
9. Wang, L., Jacquesa, S. L. & Zhengb, L. MCML - Monte Carlo modeling of light transport in multi-layered tissues. *Biomedicine* **2607**, (1995).
10. Simpson, C. R., Kohl, M., Essenpreis, M. & Cope, M. Near-infrared optical properties of ex vivo human skin and subcutaneous tissues measured using the Monte Carlo inversion technique. *Phys. Med. Biol.* **43**, 2465–2478 (1998).
11. Burkhardt, R. *et al.* Changes in trabecular bone, hematopoiesis and bone marrow vessels in aplastic anemia, primary osteoporosis, and old age: A comparative histomorphometric study. *Bone* **8**, 157–164 (1987).
12. Ugryumova, N., Matcher, S. J. & Attenburrow, D. P. Measurement of bone mineral density via light scattering. *Phys. Med. Biol.* **49**, 469–483 (2004).
13. Ascenzi, A. & Fabry, C. Technique for dissection and measurement of refractive index of osteones. *J. Biophys. Biochem. Cytol.* **6**, 139–142 (1959).
14. Lipo Wang. *Support Vector Machines: Theory and Applications. Studies in Fuzziness and Soft Computing* vol. 177 (Springer Berlin Heidelberg, 2005).

学位論文審査報告書（甲）

1. 学位論文題目（外国語の場合は和訳を付けること。）

機械学習を用いた多方向光学式骨密度計測法の開発

Development of a Multidirectional Optical Bone Densitometry Using Machine Learning Techniques

2. 論文提出者 (1) 所 属 機械科学専攻

(2) 氏 名 三浦 要

3. 審査結果の要旨（600～650字）

当該学位論文に関し、令和4年7月25日に第1回学位論文審査委員会を開催し、提出された学位論文および関連資料について詳細に審査した。同日に行われた口頭発表の後、第2回学位論文審査委員会を開催し、慎重に協議した結果、以下の通り判定した。

本研究は、骨粗鬆症の早期発見のための新たな光学式骨密度測定法を提案し、その有効性を検証することを目的とした。提案した手法は、生体組織へ近赤外光を照射した際に生じる三方向（光の照射方向に対して後方、前方、および側方）の皮膚上の拡散光強度分布データから骨密度を予測するものである。組織を構成する皮膚と骨の構造的および光学的特性を生理的範囲内でランダムに組み合わせ、健常から骨粗鬆症までの状態を再現した計1,211種類の生体組織モデルを構築し、モンテカルロ法により皮膚上の拡散光強度分布を計算した。これを機械学習させることで骨密度を予測し、交差検証を行った結果、決定係数 0.760 を得た。この結果は、提案した手法が皮膚などの軟組織の個人差に対してロバストであり、十分な骨密度予測精度を有することを示している。このことから、本手法は、X線を用いない安全で簡便な骨粗鬆症スクリーニングの新技术となり得るものであり、骨粗鬆症の予防に大きく貢献できる可能性を有していると言える。以上より、本論文は生体医工学分野における学術的価値が高く、博士（学術）に値するものと判定した。

4. 審査結果 (1) 判定（いずれかに○印） 合格 ・ 不合格

(2) 授与学位 博士（学術）